Assessment of a 6-arylaminobenzamide lead derivative as a potential core scaffold for S1P5 positron emission tomography radiotracer development

Bioorg. Med. Chem. 119 (2025) 118057

Contents lists available at ScienceDirect

Bioorganic & Medicinal Chemistry

journal homepage: www.elsevier.com/locate/bmc

Assessment of a 6-arylaminobenzamide lead derivative as a potential core scaffold for $S1P_5$ positron emission tomography radiotracer development

Robert C. Shaw [a,b], Timaeus E.F. Morgan [c], Holly McErlain [c], Carlos J. Alcaide-Corral [a,b], Adam D. Waldman [d], Dmitry Soloviev [e], David Y. Lewis [e,f], Andrew Sutherland [c], Adriana A.S. Tavares [a,b,*]

[a] University/BHF Centre for Cardiovascular Sciences, University of Edinburgh, 47 Little France Crescent, Edinburgh EH16 4TJ UK
[b] Edinburgh Imaging, University of Edinburgh, 47 Little France Crescent, Edinburgh EH16 4TJ UK
[c] School of Chemistry, University of Glasgow, University Avenue, Glasgow G12 8QQ UK
[d] Centre for Clinical Brain Sciences, University of Edinburgh, 49 Little France Crescent, Edinburgh EH16 4SB UK
[e] School of Cancer Sciences, University of Glasgow, Switchback Road, Glasgow G61 1QH UK
[f] Cancer Research UK Scotland Institute, Switchback Road, Glasgow G61 1BD UK

ARTICLE INFO

Keywords:
Sphingosine-1-phosphate-5 receptors
$S1P_5$
Radiotracer
Radiotracer development
Positron emission tomography
Aminobenzamides

ABSTRACT

Sphingosine-1-phosphate-5 receptors ($S1P_5$) are predominantly expressed in oligodendrocytes and as a result have been proposed as an important target in Multiple Sclerosis (MS). Selective $S1P_5$ radiotracers could enable *in vivo* positron emission tomography (PET) imaging of oligodendrocytes activity. Here we report the synthesis, radiolabelling and first preclinical evaluation of the pharmacokinetics and binding properties of a lead 6-arylaminobenzamide derivative, 6-(mesitylamino)-2-methoxy-3-methylbenzamide (also named as TEFM180), as a potential core scaffold for development of novel $S1P_5$ PET radiotracers. Following intravenous bolus injection, TEFM180 was found to quickly enter the brain with good brain:blood ratios and subsequent rapid clearance. Autoradiography studies showed that [^{3}H]TEFM180 had a high affinity for its target (K_D = 2.8 nM), with moderate levels of non-displaceable binding. Distribution of [^{3}H]TEFM180 in the brain was found to be consistent with $S1P_5$ expression and showed a binding potential (BP) of >2–3 in white matter rich regions. Overall, TEFM180 offers a good initial platform for development of future radiotracers targeting $S1P_5$.

1. Introduction

Multiple Sclerosis (MS) is a debilitating neuroinflammatory demyelinating disease that has no cure, however, in recent years, disease modifying therapies have been developed and approved for use.[1–3] Discovery of FTY720 (Fingolimod), the first sphingosine-1-phosphate (S1P) modulator approved for the treatment of MS, confirmed the importance of S1P receptors as a target for the treatment of MS.

$S1P_{1–5}$ receptors are G protein-coupled receptors (GPCR),[4] which have differing distributions and functions in both the periphery and the central nervous system (CNS)[5] and beyond. They are high affinity receptors for the endogenous ligand S1P (**1**) (Fig. 1).[6] The primary mechanism of action of FTY720 (**2**) is on $S1P_1$ in the lymph nodes, acting as an immunomodulator. However, FTY720 is known to bind to $S1P_1$, $S1P_3$ and $S1P_5$ in the CNS. $S1P_5$ is expressed almost exclusively on white matter (mature myelinating oligodendrocytes)[7] as well as on oligodendrocyte precursor cells within the rat CNS.[8] $S1P_5$ activation has been shown to lead to process retraction in developmental oligodendrocytes and promote cell survival in mature oligodendrocytes.[9] Due to these factors, it was proposed that compounds selective for $S1P_5$ could make excellent candidates for novel radiotracers to image oligodendrocytes *in vivo* and improve the understanding of demyelinating diseases such as MS.

Positron Emission Tomography (PET) imaging has been used in various settings to track disease activity with high levels of sensitivity and specificity, quantifying activity at the molecular level early in the

Abbreviations: MS, Multiple Sclerosis; S1P, Sphingosine-1-phosphate; $S1P_5$, Sphingosine-1-phosphate-5 receptor; GPCR, G protein-coupled receptors; CNS, Central nervous system; PET, Positron Emission Tomography; BBB, Blood brain barrier; K_D, dissociation constant; *BP*, binding potential; HPLC, High performance liquid chromatography.

* Corresponding author at: University/BHF Centre for Cardiovascular Sciences, University of Edinburgh, 47 Little France Crescent, Edinburgh EH16 4TJ, UK.
E-mail address: adriana.tavares@ed.ac.uk (A.A.S. Tavares).

https://doi.org/10.1016/j.bmc.2024.118057
Received 29 October 2024; Received in revised form 19 December 2024; Accepted 29 December 2024
Available online 3 January 2025

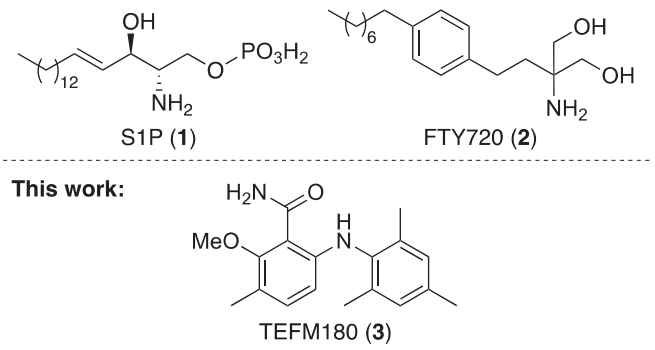

Fig. 1. Molecular Structures of S1P, FTY720 and TEFM180.

disease course.[10] This could be invaluable in MS research and the subsequent development of novel therapeutics. The first step of novel PET radiotracer development is target identification and lead compound discovery. Recognition of the most appropriate position for introduction of the positron emitting isotope is also important. In addition, a successful PET radiotracer for brain imaging needs to be able to cross the blood–brain-barrier (BBB) rapidly and display kinetics amenable to short-term framing PET imaging. In 2010, Novartis reported a library of selective $S1P_5$ agonists, including 6-(mesitylamino)-2-methoxy-3-methylbenzamide (**3**) (referred to as TEFM180), which displayed high $S1P_5$ potency and significant activity in oligodendrocytes.[11] As well as these properties, TEFM180 (**3**) showed highly selectivity for S1P5, with an EC_{50} value of 2 nM, compared to 476 nM and 373 nM for S1P1 and S1P4, respectively. Due to its high affinity and selectivity for $S1P_5$ and being amenable to carbon-11 labelling, TEFM180 (**3**) was proposed as a potential PET radiotracer. Herein, we report the synthesis, radiolabelling and preclinical evaluation of TEFM180 (**3**) as a radiotracer for SIP_5. The assessment of multi-organ and blood biodistribution, BBB penetration potential and binding properties in rat brain tissue of TEFM180 (**3**) are also described.

2. Results

2.1. Synthesis of precursor and TEFM180 (3)

The first stage of the project focused on the development of a synthetic route that would allow access to both TEFM180 (**3**) and a hydroxyl precursor that could be methylated with an appropriate radiolabel. A similar approach as described by Mattes and co-workers was used with some modifications (Scheme 1).[11] Nucleophilic aromatic substitution of 2-bromo-6-fluoro-3-methylbenzoic acid (**4**) with 2,4,6-trimethylaniline (**5**), under basic conditions gave biarylamine **6** in quantitative yield. The key hydroxyl group was introduced as a benzyl ether using a copper-catalyzed Ullmann coupling that gave ether **7** in 74 % yield. Following amidation of **7**, which gave amide **8** in 92 % yield, hydrogenation of the benzyl ether under standard conditions gave hydroxyl precursor **9** in 87 % yield. This material was methylated by NOVANDI Chemistry AB for our preclinical studies to give [^{3}H]TEFM180 (**10**) with a specific activity of 81 Ci/mmol (2.99 TBq/mmol) and a radiochemical purity of >99 %. Synthesis of TEFM180 (**3**) was completed by methylation of **9** using methyl iodide and potassium carbonate. It should be noted that this general route was designed to be highly amenable for the late-stage radiosynthesis of other TEFM180 radiotracers using various radioisotopes of methyl iodide (e.g. [^{11}C]MeI, quod vide).

2.2. TEFM180 distribution in blood versus rat brain

To determine the level of TEFM180 (**3**) concentration that can be detected, a HPLC study was conducted. TEFM180 (**3**) was found to have

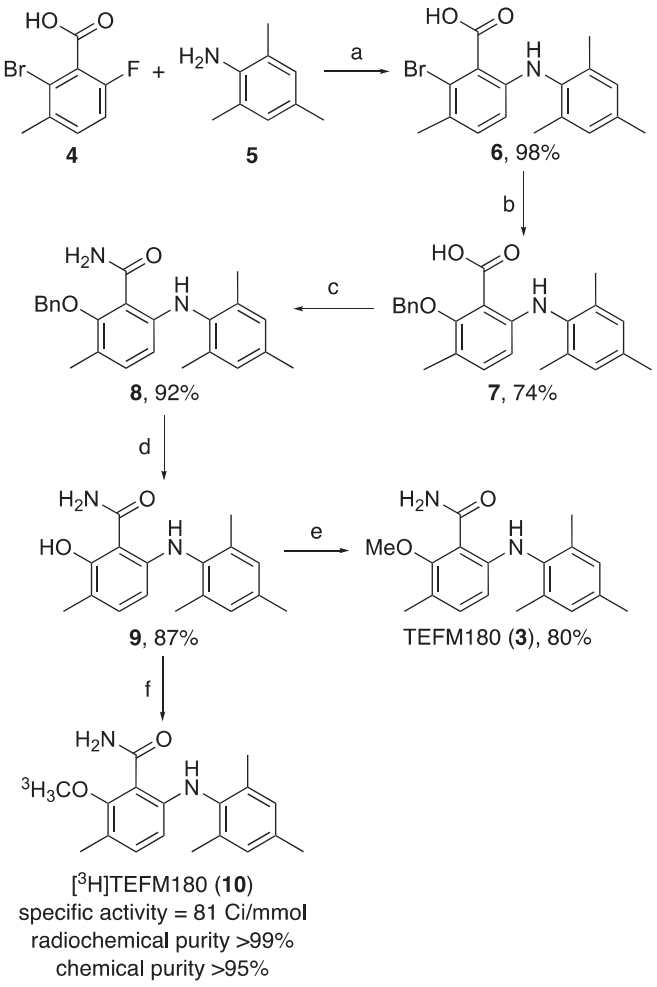

Scheme 1. Synthesis of precursor, TEFM180 (**3**) and [^{3}H]TEFM180 (**10**).[a] [a]Reagents and conditions: (a) LiHMDS, THF, −78 to 40 °C, 16 h, 98 %; (b) BnOH, Cu (40 mol%), NaH, THF, 0–80 °C, 24 h, 74 %; (c) 2-chloro-4,6-dimethoxy-1,3,5-triazine, NMM, NH_4OH, THF, rt, 2 h, 92 %; (d) H_2, 10 % Pd/C, THF, rt, 2 h, 87 %; (e) MeI, K_2CO_3, acetone, rt to 40 °C, 16 h, 80 %; (f) KOH, DMSO, rt, 0.25 h, then [^{3}H]MeI in DMSO, 80 °C, 0.5 h.

a consistent HPLC retention time (6.57 ± 0.02 min) both within and between runs with good intermediate precision results of 0.3 %. Using signal to noise ratio analysis, the lowest concentration of TEFM180 (**3**) that could be detected was 0.05 μg/mL with a signal to noise ratio of 2.65 (Fig. 2).

Following intravenous bolus injection, there was a rapid distribution of TEFM180 (**3**) from the blood to the tissue over the first 30 min and a slower clearance at later time points up to 240 min (Fig. 3). The blood data followed a biphasic exponential decay kinetics (Fig. 3A), displaying a fast half-life of 0.25 min followed by a slow half-life of 15.62 min. A high uptake of TEFM180 (**3**) into the brain was measured at 30 min post-injection, second only to the amount in the lungs (Fig. 3B). It can also be observed that the amount of TEFM180 (**3**) decreased through the time points and cleared from the tissue. TEFM180 (**3**) concentration in brain was greater than in blood at all measurement time points (Fig. 3C) and the average brain:blood ratio was >2 at 30 min post-injection of TEFM180 (**3**) (Fig. 3D).

2.3. [^{3}H]TEFM180 (10) specific binding in rat brain tissue sections

[^{3}H]TEFM180 (**10**) had low to moderate specific binding in rat brain tissue sections and this binding is dose dependent (Fig. 4). Estimated K_D of [^{3}H]TEFM180 (**10**) was 2.8 nM and 0.6 nM at room temperature

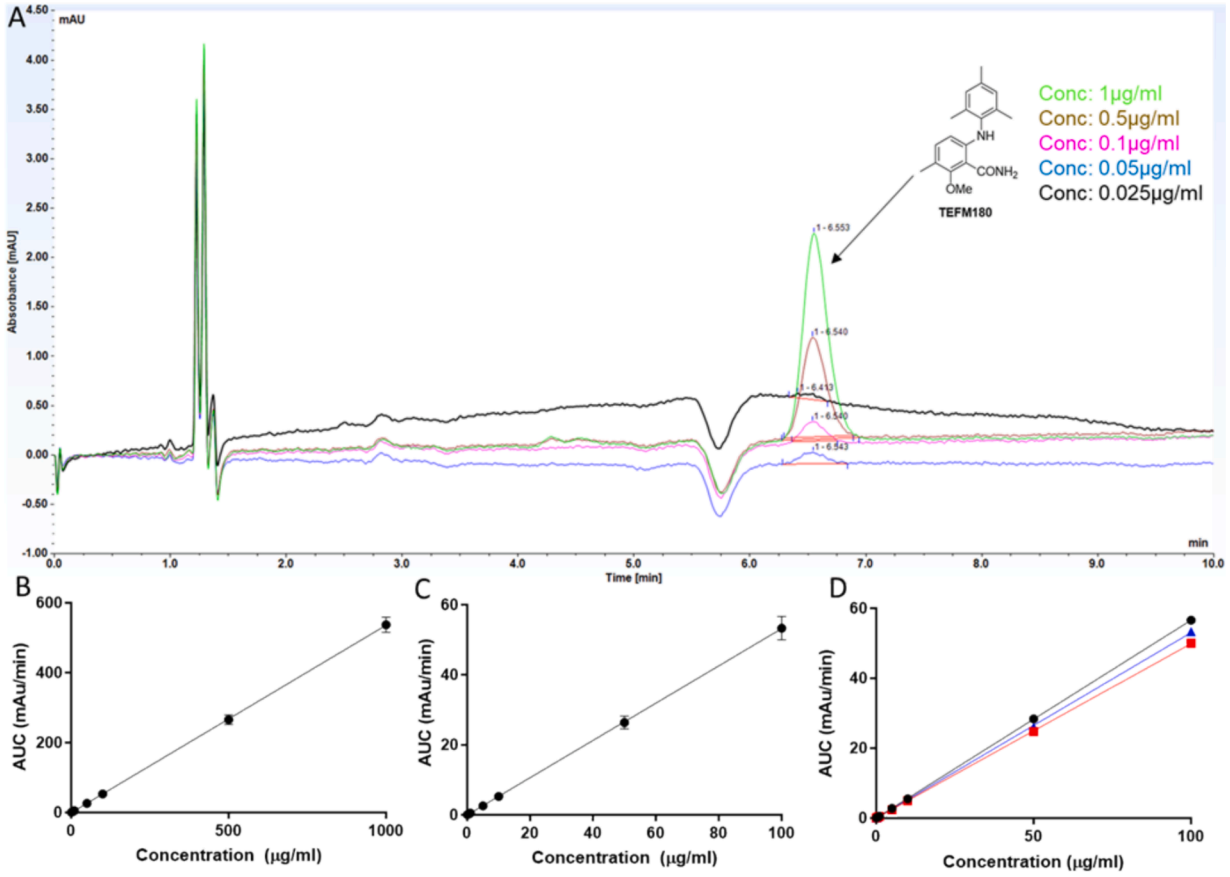

Fig. 2. Example chromatograms and calibration curves for TEFM180 **(3)**. (A) Chromatograms for TEFM180 (**3**) from 0.01 µg/mL to 1 µg/mL. (B) Calibration curve containing all assessed data points from 0.01 µg/mL to 1000 µg/mL (mean ± SEM, n = 3) and (C) from 0.01 µg/mL to 100 µg/mL (mean ± SEM, n = 3) demonstrating a linear relationship between points. (D) The calibration curve at lower concentrations split into the three separate days of assessment to show variation between runs.

(Fig. 4B) and 37 °C (Fig. 4C), respectively. This is consistent with previous studies showing that an increase of K_D at physiological temperatures is expected in binding studies.[12]

2.4. [^{3}H]TEFM180 (**10**) distribution in rat brain versus $S1P_5$ expression

The highest binding of [^{3}H]TEFM180 (**10**) was measured in the midbrain and corpus callosum (Fig. 5A–C), which are white matter rich regions known to contain high levels of $S1P_5$.[7] The average % specific binding across various brain regions was around 60 %, except for the forceps minor, which had a % specific binding of around 20 % (Fig. 5D). This shows a moderate level of non-displaceable binding (Fig. 5E). The regional brain distribution of [^{3}H]TEFM180 in rat tissue sections is consistent with previous immunostaining studies in the same species, showing greatest density of $S1P_5$ positive cells in the corpus callosum and anterior commissure, followed by neocortex, striatum and septum and thalamus.[8]

Measured B_{avail} for different brain regions with [^{3}H]TEFM180 (**10**) ranged between ~1700 fmol/mg and 9600 fmol/mg (Table 1). Using established K_D at room temperature of 2.8 nM, the *BP* was estimated to range between 0.64 and 3.48.

2.5. Radiosynthesis of [^{11}C]TEFM180

Having shown that TEFM180 (**3**) has favorable pharmacokinetics, a preliminary study was conducted to evaluate the suitability of compound **9** for radiolabelling using carbon-11 methyl iodide (Scheme 2). [^{11}C]MeI was synthesized from [^{11}C]CO_2 by the gas-phase method using the bespoke modification of the Synthra automated radiosynthesizer.[13] From approximately 10 GBq of [^{11}C]CO_2, 5 GBq of [^{11}C]MeI was produced 10 min after the end of bombardment. For an optimal ^{11}C-methylation, various bases were then screened. The use of sodium hydroxide, potassium carbonate or tetra-*n*-butylammonium hydroxide in THF at various temperatures (40–80 °C) gave low conversion (<5%) after a 10-minute reaction time, with carbon-11 methanol as the main by-product. Switching to tetra-*n*-butylammonium fluoride (TBAF) and bubbling [^{11}C]MeI directly into the preheated precursor solution led to a significantly improved outcome, due to a favorable increase of methylation reaction kinetics over basic hydrolysis of MeI. At 80 °C and a 5-minute reaction time gave 72 % conversion. Further studies identified cyclohexanone as the optimal solvent and a reaction temperature of 120 °C. This gave [^{11}C]TEFM180 in 94 % conversion. Purification of [^{11}C]TEFM180 was then achieved using semi-preparative HPLC, and following reformulation, this gave the product in 13 % activity yield after a total synthesis time of 63 min and >99 % radiochemical purity.

3. Discussion

The aim of this study was to assess the binding properties of [^{3}H]TEFM180 (**10**) in rat brain tissue *in vitro* and determine the multi-organ and blood kinetics of TEFM180 *in vivo*. Data showed that TEFM180 (**3**) can penetrate the BBB, has blood and brain kinetics amenable for PET imaging, and that [^{3}H]TEFM180 (**10**) distribution in rat brain tissue sections is consistent with $S1P_5$ expression.

It was found that [^{3}H]TEFM180 (**10**) can be detected at low concentrations using HPLC due to its strong UV absorbance and consistent retention time. When formulated in DMSO and administered via the intravenous route, [^{3}H]TEFM180 (**10**) enters the brain. The

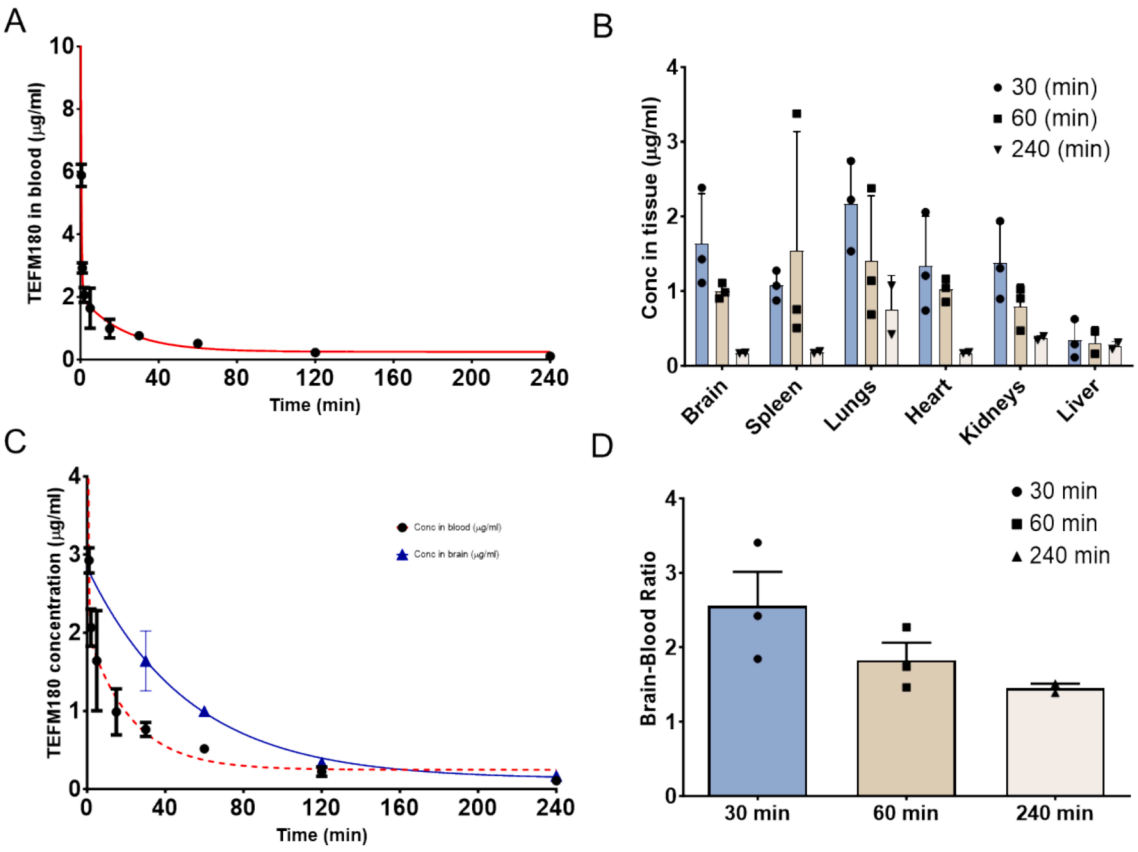

Fig. 3. TEFM180 (**3**) concentration in rat blood and tissue over time. (A) Concentration of TEFM180 (**3**) shows rapid distribution from the blood over the first 30 min post injection, followed by a slower distribution up to 240 min (mean ± SEM, n = 2–7; $T_{1/2fast}$ = 0.25 min and a $T_{1/2slow}$ = 15.62 min). (B) TEFM180 (**3**) concentration across organs at 30-, 60- and 240-minutes post injection. (C) TEFM180 (**3**) shows moderate clearance from the brain over 240 min (mean ± SEM, n = 1–3). (D) Brain to blood ratio of TEFM180 (**3**) decreases over time however the concentration in the brain is greater than in the blood at each time point.

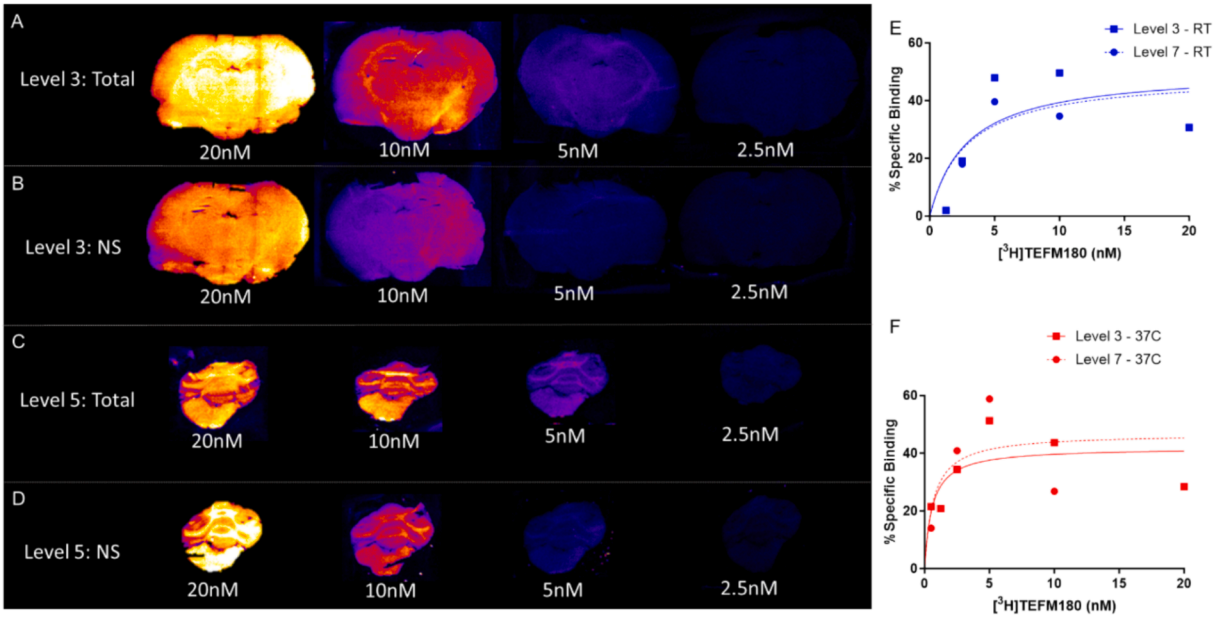

Fig. 4. Saturation binding assays using [^{3}H]TEFM180 (**10**) autoradiography. (A–B) Total binding slides for level 3 and level 5 at various radioactive concentrations. (C–D) Non-specific binding slides for level 3 and level 5 at various radioactive concentrations. (E) Saturation binding assay plot for binding at room temperature (one-site total binding is the preferred model over two site specific binding, $p < 0.0001$). (F) Saturation binding assay plot for binding at 37 °C (one-site total binding is the preferred model over two site specific binding, $p < 0.0001$).

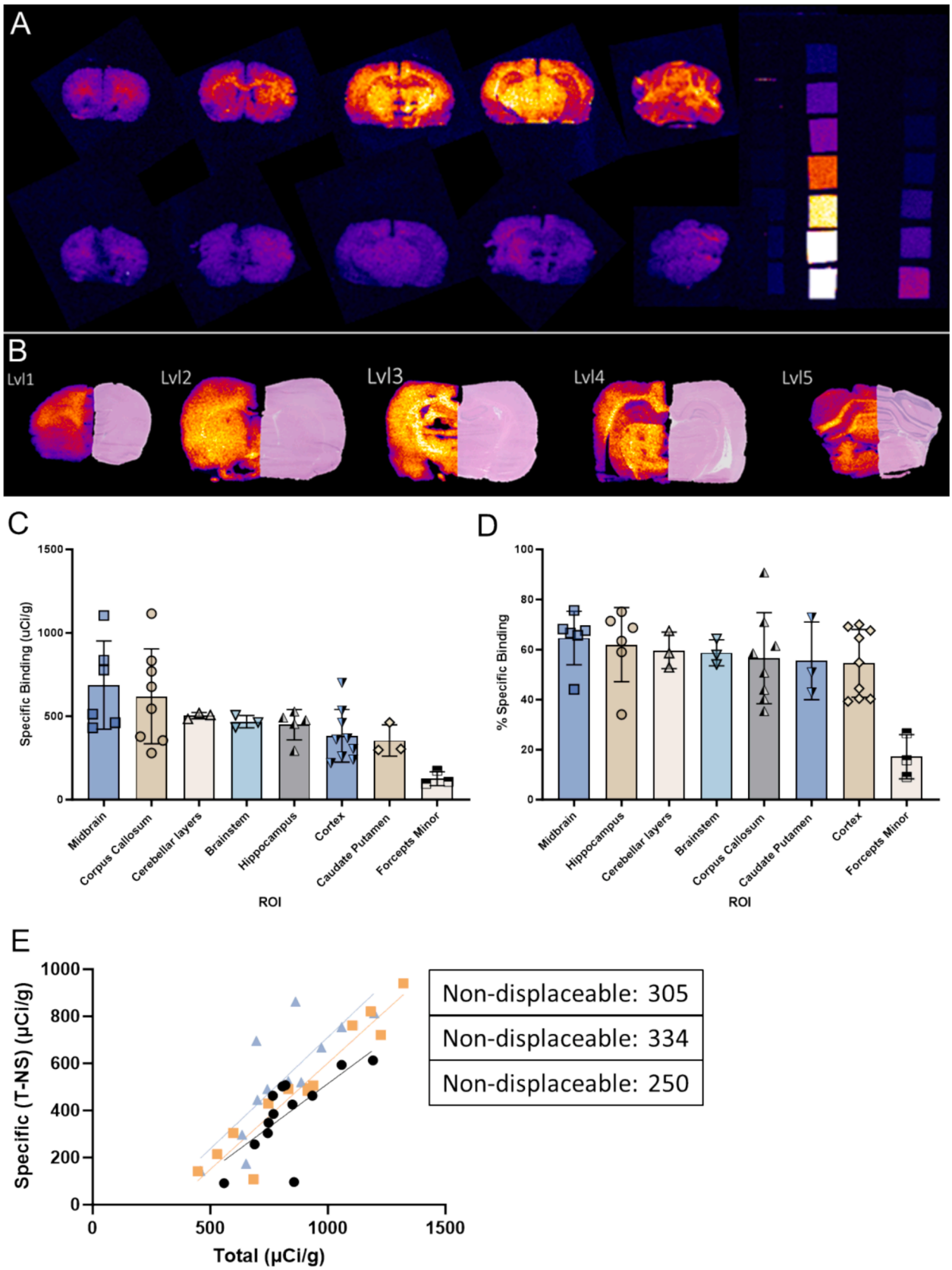

Fig. 5. Specific and non-displaceable binding from [^{3}H]TEFM180 (**10**) autoradiography. (A) Total binding (top) and non-specific slides with scales to the right allowing for quantification of the signal. (B) Example autoradiography images merged with hematoxylin and eosin (H&E) sections from serial sections. (C) Specific binding across brain regions. (D) Percent specific binding across brain regions. Data in panels C and D presented as mean ± SD, n = 3 rats and n = 3–9 measurements per region (ROIs that are present across levels). (E) Lassen plot for each individual rat showing the non-displaceable binding.

Table 1
[^{3}H]TEFM180 (**10**) regional brain distribution and binding properties determined using rat brain tissue autoradiography. Data presented as mean ± SD (n = 3). K_D = dissociation constant, BP = binding potential.

Brain region	Binding (fmol/mg)	Binding (nM)	K_D (nM)	*BP*
Forcepts Minor	1767.81 ± 478.27	1.79 ± 0.48	2.8	0.64 ± 0.17
Corpus Callosum	8444.04 ± 1581.21	8.53 ± 1.6	2.8	3.05 ± 0.57
Caudate Putamen	4992.4 ± 1073.25	5.04 ± 1.08	2.8	1.8 ± 0.39
Cortex	5385.59 ± 750.74	5.44 ± 0.76	2.8	1.94 ± 0.27
Hippocampus	6414.19 ± 703.24	6.48 ± 0.71	2.8	2.31 ± 0.25
Midbrain	9659.57 ± 2713.35	9.76 ± 2.74	2.8	3.48 ± 0.98
Cerebellar layers	7084.21 ± 212.76	7.16 ± 0.21	2.8	2.56 ± 0.08
Brainstem	6573.04 ± 425	6.64 ± 0.43	2.8	2.37 ± 0.15
Average all regions	6298.3 ± 505.3	6.36 ± 0.51	2.8	2.27 ± 0.18

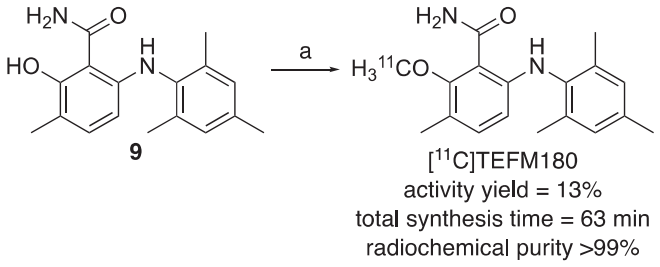

Scheme 2. Radiosynthesis of [^{11}C]TEFM180.[a] [a]Reagents and conditions: (a) [^{11}C]MeI, TBAF (1 M in THF), cyclohexanone, 120 °C, 3 min.

biodistribution of [^{3}H]TEFM180 (**10**) analogues were tested by Mattes and co-workers[11] using an oral administration with NMP/Solutol/PEG-300 (5:10:85 v/v/v) formulations or the intravenous route with the NMP/PEG (5:95 v/v) formulations. In the original paper and formulation, [^{3}H]TEFM180 (**10**) analogues were found to have a half-life in rat plasma ranging between 2.8 and 7.4 h. Although long-lived PET isotopes could be considered for labelling of these compounds, to be compatible with PET imaging requirements, an ideal PET radiotracer would be developed using shorter-lived isotopes with better dosimetry profile. In our study, TEFM180 (**3**) had a much faster half-life (minutes rather than hours) in rat plasma when administered intravenously, which is suitable for PET imaging radiotracer development. The differences in kinetics are likely due to the variance in formulation used and compound structure.

Agonist compounds can display quasi irreversible binding kinetics, which can be problematic for a PET imaging biomarker, as observed with some $5HT_{1A}$ agonist radiotracers.[14] Furthermore, it is known that FTY720 causes internalization at the $S1P_1$ receptor, which is responsible for its therapeutic effect of preventing release of immune cells from the lymph nodes.[15] To determine if TEFM180 (**3**) binding kinetics would be compliant with PET imaging, we investigated its biodistribution and kinetics *in vivo* and *in vitro*. We found that its clearance and elimination properties are not consistent with internalization or quasi-irreversible kinetics. Therefore, it is a suitable scaffold for $S1P_5$ PET radiotracer development. The estimated K_D for TEFM180 (**3**) at room temperature was 2.8 nM, which is consistent with that found for $S1P_5$ affinity analysis using $GTP_\gamma S$ assays in cell lines overexpressing the human S1P receptors in the Novartis paper (EC_{50} = 2 nM for $S1P_5$).[11] This is a good K_D value for a brain PET tracer and compares favorably with previously developed radiotracers.[16] This affinity value enables good target engagement, while minimizing potential for internalization and quasi-irreversible kinetics, therefore corroborating the pharmacokinetics analysis showing TEFM180 is a suitable scaffold for $S1P_5$ PET radiotracer development.

Data from the autoradiography showed that the corpus callosum had the highest levels of [^{3}H]TEFM180 (**10**) specific binding and B_{avail}. High specific binding in other white matter rich regions was also observed, namely, midbrain, brainstem and cerebellum layers. This binding is in line with previous $S1P_5$ literature using *in situ* hybridization which showed $S1P_5$ mRNA was primarily expressed in white matter tracts in rat brain tissue; the corpus callosum, midbrain structures and cerebellar white matter matched [^{3}H]TEFM180's binding pattern.[7,8]

Results showed that [^{3}H]TEFM180 (**10**) had moderate non-specific binding, which might be attributed to its high lipophilicity (log *P* of 4.23). Moderately high lipophilicity enables passive entry across the BBB, but can to lead to high plasma protein binding.[17] Once in the brain, highly lipophilic radiotracers are also more likely to have high levels of non-specific binding in the brain[18–20] as 60 % of the brain's dry weight is composed of lipids.[21] Therefore, high non-specific binding to lipids in the brain may have contributed to an overly high estimation of B_{avail} for [^{3}H]TEFM180 (**10**).

The calculated *BP* for [^{3}H]TEFM180 (**10**) for the whole rat brain tissue section was on average 2.16. Typically a *BP* of >5 is considered optimal for quantitative PET imaging,[16] although many radiotracers have been successful in the clinic with BP values of 0.5 to 1.5.[16] The [^{3}H]TEFM180 (**10**) *BP*, albeit not ideal, provides a good starting point and platform for subsequent $S1P_5$ radiotracer development programmes. The next steps for this programme of research would be to optimize radiotracer properties for easy widespread clinical translation, including exploring new TEFM180 analogues amenable to fluoride-18 labelling. The subsequent hit compound could then be used to conduct preclinical imaging studies in rodent models of MS.

4. Conclusions

In summary, a synthetic approach has been developed for the preparation of a 6-arylaminobenzamide derivative, TEFM180 (**3**) and its hydroxyl precursor, which was subsequently used to generate a tritium-labelled analogue. Both compounds were used to conduct the first preclinical evaluation of this motif and our findings indicate that TEFM180 (**3**) can serve as a successful core scaffold for development of $S1P_5$ PET radiotracers. Firstly, TEFM180 (**3**) has favorable pharmacokinetics for a short-lived radiotracer. Additionally, its strong affinity in rat brain tissue and distribution pattern consistent with previous reports of $S1P_5$ makes it a viable candidate for further development. Furthermore, a preliminary study demonstrated that [^{11}C]TEFM180 was amenable to convenient automated radiosynthesis, hence, suggesting that other analogues could be prepared in a similar manner. TEFM180 (**3**) demonstrates moderate specific binding with a high level of non-displaceable binding, likely due to high lipophilicity. Therefore, future research will focus on exploring TEFM180 (**3**) analogues with improved lipophilicity properties while maintaining good structure–activity relationships with the target receptor. The Novartis study reported a 3-chloro-6-arylaminobenzamide with high potency and selectivity for $S1P_5$ that is likely to be less lipophilic than TEFM180 (**3**).[11] Thus, future targets will explore the incorporation of small, hydrophilic 3-substituents, with the aim of improving the overall lipophilicity of potential PET imaging agents for $S1P_5$.

5. Experimental section

All reagents and starting materials were obtained from commercial sources and used as received. All reactions were performed under an atmosphere of air unless otherwise stated. All dry solvents were purified using a PureSolv 500 MD solvent purification system. Brine is defined as a saturated solution of aqueous sodium chloride. Flash column chromatography was carried out using Merck Geduran Si 60 (40–63 μm).

Merck aluminium-backed plates pre-coated with silica gel 60 (UV_{254}) were used for thin layer chromatography and were visualized under ultraviolet light and by staining with $KMnO_4$, ninhydrin or vanillin. ^1H NMR and ^{13}C NMR spectra were recorded on a Bruker DPX 400 spectrometer with chemical shift values in ppm relative to tetramethysilane (δ_H 0.00 and δ_C 0.0) or residual chloroform (δ_H 7.26 and δ_C 77.2) as the standard. Assignment of ^1H and ^{13}C NMR signals are based on 2-dimensional COSY, HSQC and DEPT experiments. Infrared spectra were recorded using a Shimadzu FTIR-84005 spectrometer and mass spectra were obtained using a JEOL JMS-700 spectrometer or a Bruker MicroTOFq high resolution mass spectrometer. Melting points were determined on a Gallenkamp melting point apparatus. Final compounds were analyzed using a Shimadzu reverse-phase HPLC system with a Kinetex® 5 μm EVO C18 100 Å column (250 × 4.6 mm) and UV detection at 254 nm. The mobile phase for analysis was a gradient of 10–90 % acetonitrile in water with 0.1 % trifluoroacetic acid at a flow rate of 1 mL/minute. Purity of all final compounds is >95 %, as determined by HPLC.

5.1. 2-Bromo-6-(mesitylamino)-3-methylbenzoic acid (6)

2-Bromo-6-fluoro-3-methylbenzoic acid (**4**) (2.00 g, 8.58 mmol) was dissolved in tetrahydrofuran (50 mL) under an atmosphere of argon. 2,4,6-Trimethylaniline (**5**) (2.60 mL, 17.2 mmol) was added and the mixture cooled to −78 °C. Lithium bis(trimethylsilyl)amide (25.7 mL, 25.7 mmol, 1.0 M in tetrahydrofuran) was slowly added over 0.1 h. The reaction mixture was allowed to reach room temperature before heating to 40 °C and stirring for 16 h. The reaction was quenched with water (25 mL), acidified to pH 2 with 10 % aqueous hydrochloric acid and then extracted with ethyl acetate (3 × 25 mL). The combined organic layer was dried ($MgSO_4$), filtered and concentrated *in vacuo*. Purification by flash column chromatography, eluting with 20–40 % ethyl acetate in petroleum ether (40–60) gave 2-bromo-6-(mesitylamino)-3-methylbenzoic acid (**6**) as a brown solid (2.84 g, 98 %). Mp 142–144 °C; IR (neat) 3415, 2915, 1674, 1600, 1560, 1485, 1288, 1232, 1107, 1012, 854, 816 cm^{-1}; ^1H NMR (400 MHz, $CDCl_3$): δ 9.26 (br s, 1H, OH), 7.00 (d, 1H, J = 8.5 Hz, 4-H), 6.96 (s, 2H, 3'-H and 5'-H), 6.14 (d, 1H, J = 8.5 Hz, 5-H), 2.33 (br s, 6H, 3-CH_3 and 4'-CH_3), 2.17 (s, 6H, 2'-CH_3 and 6'-CH_3); $^{13}C\{^1H\}$ NMR (101 MHz, $CDCl_3$): δ 173.5 (C), 146.2 (C), 136.03 (C), 136.01 (2 × C), 134.6 (C), 133.8 (CH), 129.4 (2 × CH), 127.7 (C), 124.0 (C), 117.4 (C), 112.3 (CH), 23.0 (CH_3), 21.0 (CH_3), 18.2 (2 × CH_3); MS (ESI) *m/z* 346 [$(M-H)^-$, 100 %]; HRMS (ESI) *m/z*: $([M-H]^-$ Calcd for $C_{17}H_{17}^{79}BrNO_2$ 346.0448; Found 346.0450.

5.2. 2-(Benzyloxy)-6-(mesitylamino)-3-methylbenzoic acid (7)

To a suspension of sodium hydride (1.15 g, 28.7 mmol) in tetrahydrofuran (16 mL) at 0 °C under argon was added dropwise benzyl alcohol (2.96 mL, 28.7 mmol) and the resulting solution stirred for 0.5 h. 2-Bromo-6-(mesitylamino)-3-methylbenzoic acid (**6**) (2.00 g, 5.74 mmol) and copper powder (0.146 g, 2.30 mmol) were then added and the reaction mixture stirred at 80 °C for 24 h. The reaction mixture was cooled to room temperature and filtered through a pad of Celite®. The filtrate was concentrated *in vacuo* and diluted in water (20 mL). The mixture was acidified to pH 2 using 10 % aqueous hydrochloric acid and extracted with dichloromethane (3 × 30 mL). The combined organic layer was dried ($MgSO_4$), filtered and concentrated *in vacuo*. Purification by flash column chromatography, eluting with 10 % ethyl acetate in petroleum ether (40–60) gave 2-(benzyloxy)-6-(mesitylamino)-3-methylbenzoic acid as a brown solid (**7**) (1.60 g, 74 %). Mp 89–91 °C; IR (neat) 3294, 2916, 1697, 1501, 1396, 1381, 1223, 1034, 814, 698 cm^{-1}; ^1H NMR (400 MHz, $CDCl_3$): δ 12.09 (br s, 1H, OH), 9.47 (br s, 1H, NH), 7.58–7.36 (m, 5H, Ph), 7.03 (d, 1H, J = 8.8 Hz, 4-H), 6.94 (s, 2H, 3'-H and 5'-H), 6.05 (d, 1H, J = 8.8 Hz, 5-H), 4.97 (s, 2H, CH_2Ph), 2.31 (s, 3H, CH_3), 2.28 (s, 3H, CH_3), 2.13 (s, 6H, 2'-CH_3 and 6'-CH_3); $^{13}C\{^1H\}$ NMR (101 MHz, $CDCl_3$): δ 168.6 (C), 156.6 (C), 150.6 (C), 137.0 (CH), 136.6 (2 × C), 136.3 (C), 134.42 (C), 134.40 (C), 129.3 (CH), 129.2 (2 × CH), 128.98 (2 × CH), 128.95 (2 × CH), 116.4 (C), 110.2 (CH), 102.7 (C), 77.6 (CH_2), 21.0 (CH_3), 18.1 (2 × CH_3), 15.4 (CH_3); MS (ESI) *m/z* 398 ($M + Na^+$, 100 %); HRMS (ESI) *m/z*: $[M + Na]^+$ Calcd for $C_{24}H_{25}NNaO_3$ 398.1727; Found 398.1712.

5.3. 2-(Benzyloxy)-6-(mesitylamino)-3-methylbenzamide (8)

2-(Benzyloxy)-6-(mesitylamino)-3-methylbenzoic acid (**7**) (1.60 g, 4.26 mmol) was dissolved in tetrahydrofuran (15 mL) and 2-chloro-4,6-dimethoxy-1,3,5-triazine (0.897 g, 5.11 mmol) and *N*-methylmorpholine (1.41 mL, 12.8 mmol) were added. The mixture was then stirred for 2 h at room temperature. The precipitate was filtered and ammonium hydroxide (35 mL) was added to the filtrate. The reaction mixture was stirred for 0.5 h at room temperature and then filtered. 2 M Sodium hydroxide (40 mL) was added to the filtrate and the crude product was extracted with ethyl acetate (3 × 40 mL). The combined organic layer was dried ($MgSO_4$), filtered and concentrated *in vacuo*. Purification by flash column chromatography, eluting with 10 % ethyl acetate in petroleum ether (40–60) gave 2-(benzyloxy)-6-(mesitylamino)-3-methylbenzamide (**8**) as a white solid (1.37 g, 92 %). Mp 122–124 °C; IR (neat) 3451, 3260, 2916, 1651, 1574, 1495, 1366, 1261, 1040, 912, 743 cm^{-1}; ^1H NMR (400 MHz, $CDCl_3$): δ 9.32 (br s, 1H, NH), 7.86 (br s, 1H, NH), 7.54–7.33 (m, 5H, Ph), 6.95 (d, 1H, J = 8.6 Hz, 4-H), 6.93 (s, 2H, 3'-H and 5'-H), 5.99 (d, 1H, J = 8.6 Hz, 5-H), 5.65 (br s, 1H, NH), 4.87 (s, 2H, CH_2Ph), 2.30 (s, 3H, CH_3), 2.22 (s, 3H, CH_3), 2.17 (s, 6H, 2'-CH_3 and 6'-CH_3); $^{13}C\{^1H\}$ NMR (101 MHz, $CDCl_3$): δ 170.8 (C), 156.6 (C), 149.3 (C), 136.5 (C), 136.4 (2 × C), 135.6 (C), 135.4 (C), 134.9 (CH), 129.0 (2 × CH), 128.7 (2 × CH), 128.5 (CH), 128.1 (2 × CH), 117.6 (C), 109.5 (CH), 107.3 (C), 76.1 (CH_2), 20.9 (CH_3), 18.2 (2 × CH_3), 15.5 (CH_3); MS (ESI) *m/z* 397 ($M + Na^+$, 100 %); HRMS (ESI) *m/z*: $[M + Na]^+$ Calcd for $C_{24}H_{26}N_2NaO_2$ 397.1886; Found 397.1871.

5.4. 2-Hydroxy-6-(mesitylamino)-3-methylbenzamide (9)

To a solution of 2-(benzyloxy)-6-(mesitylamino)-3-methylbenzamide (**8**) (1.36 g, 3.63 mmol) in tetrahydrofuran (100 mL) was added 10 % palladium on carbon (0.770 g) and the reaction mixture purged under hydrogen gas for 1 h, before stirring at room temperature under a hydrogen atmosphere for a further 1 h. The reaction mixture was then filtered through Celite®, washed with ethyl acetate (50 mL) and the filtrate was concentrated *in vacuo*. Purification by flash column chromatography, eluting with 10–20 % ethyl acetate in petroleum ether (40–60) gave 2-hydroxy-6-(mesitylamino)-3-methylbenzamide[9] as a white solid (0.900 g, 87 %). Mp 145–147 °C; IR (neat) 3298, 2914, 1645, 1612, 1587, 1422, 1244, 1225, 1040, 912, 802, 741 cm^{-1}; ^1H NMR (400 MHz, $CDCl_3$): δ 12.72 (s, 1H, OH), 7.50 (br s, 2H, NH_2), 6.94 (d, 1H, J = 8.1 Hz, 4-H), 6.93 (s, 2H, 3'-H and 5'-H), 5.87 (d, 1H, J = 8.1 Hz, 5-H), 5.24 (br s, 1H, NH), 2.30 (s, 3H, CH_3), 2.15 (s, 3H, CH_3), 2.13 (s, 6H, 2'-CH_3 and 6'-CH_3); $^{13}C\{^1H\}$ NMR (101 MHz, $CDCl_3$): δ 173.5 (C), 161.2 (C), 144.1 (C), 136.2 (C), 134.7 (C), 134.6 (CH), 132.7 (2 × C), 129.6 (2 × CH), 119.9 (C), 108.1 (CH), 105.2 (C), 20.8 (CH_3), 18.1 (2 × CH_3), 15.5 (CH_3); MS (ESI) *m/z* 307 ($M + Na^+$, 100 %); HRMS (ESI) *m/z*: $[M + Na]^+$ Calcd for $C_{17}H_{20}N_2NaO_2$ 307.1417; Found 307.1409.

5.5. 6-(Mesitylamino)-2-methoxy-3-methylbenzamide (3)

2-Hydroxy-6-(mesitylamino)-3-methylbenzamide (**9**) (0.015 g, 0.053 mmol) was dissolved in acetone (1 mL). Potassium carbonate (0.022 g, 0.16 mmol) and iodomethane (4.0 mL, 0.064 mmol) were added and the reaction mixture was then stirred at room temperature for 3 h. A further quantity of iodomethane (4.0 mL, 0.064 mmol) was added and the reaction mixture was heated to 40 °C for 16 h. The reaction mixture was filtered and concentrated *in vacuo*. The filtrate was suspended in water (5 mL) and extracted with dichloromethane (3 × 40 mL). The combined organic layer was dried ($MgSO_4$), filtered and concentrated *in vacuo*. Purification by flash column chromatography,

eluting with 20 % ethyl acetate in petroleum ether (40–60) gave 6-(mesitylamino)-2-methoxy-3-methylbenzamide (TEFM180, **3**) (0.013 g, 80 %). Mp 131–133 °C; IR (neat) 3468, 3228, 2913, 1626, 1571, 1496, 1407, 1370, 1264, 1152, 1046, 824, 704 cm^{-1}; ^{1}H NMR (400 MHz, $CDCl_3$): δ 9.38 (br s, 1H, NH), 7.93 (br s, 1H, NH), 6.97–6.89 (m, 3H, 4-H, 3'-H and 5'-H), 5.97 (d, 1H, $J = 8.6$ Hz, 5-H), 5.90 (br s, 1H, NH), 3.79 (s, 3H, OCH_3), 2.31 (s, 3H, CH_3), 2.17 (s, 3H, CH_3), 2.16 (s, 6H, 2'-CH_3 and 6'-CH_3); $^{13}C\{^{1}H\}$ NMR (101 MHz, $CDCl_3$): δ 170.9 (C), 158.1 (C), 149.3 (C), 136.4 (2 × C), 135.5 (C), 135.4 (C), 134.9 (CH), 129.0 (2 × CH), 117.3 (C), 109.3 (CH), 106.8 (C), 61.1 (CH_3), 20.9 (CH_3), 18.2 (2 × CH_3), 15.2 (CH_3); MS (ESI) *m/z* 299 ($M + H^+$, 100 %); HRMS (ESI) *m/z*: $[M + H]^+$ Calcd for $C_{18}H_{23}N_2O_2$ 299.1754; Found 299.1758.

5.6. Radioligand preparation

[^{3}H]TEFM180 (**10**) was custom synthesized by NOVANDI Chemistry AB (Sweden) using 2-hydroxy-6-(mesitylamino)-3-methylbenzamide (**9**) prepared in our lab, at a specific activity of 81 Ci/mmol (2.99 TBq/mmol). The radiosynthesis of [^{3}H]TEFM180 (**10**) was accomplished with a radiochemical purity of >99 %, a chemical purity of >95 % and a radioactive concentration of 1.0 mCi/mL (38 MBq/mL) in ethanol.

5.7. Animals

All experiments reported were conducted in accordance with the local University of Edinburgh animal ethics committee and were authorized by the Home Office under the Animals (Scientific Procedures) Act 1986, UK. Eleven adult male Sprague-Dawley rats (10–12 weeks, weight 389.6 ± 53.6 g) were used for the pharmacokinetics experiments. Three adult male Sprague Dawley rats (9–10 weeks old, 346.33 ± 27.34 g) were used for autoradiography experiments.

5.8. In vivo pharmacokinetic studies in rats

Animals' anaesthesia was induced using 3 % isoflurane (Isoflo, APIECE) in 50/50 oxygen/nitrous oxide and 1 L/min. Anaesthesia was maintained with 2–2.5 % isoflurane in 50/50 oxygen/nitrous oxide and 1 L/min via a nose cone. The rat femoral artery was canulated (PE50 inside diameter 0.58 mm, outside diameter 0.96 mm, and length 40 cm) to allow for the collection of arterial blood. A bolus of 5 mg/Kg of TEFM180 (**3**) diluted in 100 μL of dimethyl sulfoxide was injected through the tail vein. One millilitre of arterial blood was collected at each time point in a heparinized syringe (20 IU) (heparin from Braun Medical Inc, UK) and separated out into three different heparinized Eppendorf tubes (330 μL of blood in each). The separation of the blood into 3 separate Eppendorf tubes allowed them to be processed independently for high performance liquid chromatography (HPLC) analysis to give three blood measurements for each time point in each animal to assess the intermediate precision of the measured drug concentrations. At 30 min, 60 min or 240 min, the rats were culled, and the organs (brain, spleen, heart, liver, lungs, and kidneys) were collected. All samples were then stored in a –80 °C freezer until later analysis by HPLC.

5.9. Quantification of TEFM180 concentration in rat blood and organs

Quantification of TEFM180 (**3**) concentrations in rat blood and organs was carried out using HPLC. First, the HPLC method was established using the following conditions: mobile phase was 70 % acetonitrile with 30 % distilled water under isocratic conditions with a flow rate of 1 mL/min. The stationary phase was a Luna 10 μm C18(2) 100 Å 150 × 4.6 mm column (Phenomonex, USA). The column oven was set to 25 °C and the UV wavelength was 245 nm. An injection volume of 20 μL of TEFM180 (**3**) dilutions was injected and the run was completed over 10 min. The HPLC experiments were conducted 3 times on three separate days using freshly prepared dilutions. The signal to noise ratio, estimated as the level of peak signal divided by the background level, was calculated with values >2 considered detectable. Furthermore, the intermediate precision of retention times was estimated as the standard deviation divided by the mean times 100. After establishing the HPLC method, blood and organ samples collected during the *in vivo* TEFM180 (**3**) pharmacokinetics studies in rats were removed from the −80 °C freezer and allowed to defrost for subsequent HPLC analysis. The organs were placed on wet ice to defrost more slowly allowing time to process the blood. Once defrosted, the blood samples were spun down in a centrifuge (Heraeus Megafuge 8R Centrifuge, Thermo Scientific, UK) at 2000 g for 4 min at 4 °C. The supernatant was then pipetted off and mixed with 1.4 times its volume of acetonitrile and spun down again at 2000 g for 4 min at 4 °C. This final deproteinated supernatant was then pipetted into HPLC vials and ran using high performance liquid chromatography (HPLC) and a sample volume of 100 μL. Once defrosted, each organ was individually weighed, cut down into small pieces and an equal weight of water was then added to allow for homogenization (IKA homogenizer, Merck, USA). Once fully homogenized, acetonitrile was added in a ratio of 1.4 times the volume of the tissue homogenate to deproteinate the sample. The samples were then spun down on a centrifuge at 2000*g* for 4 min. This supernatant was collected and pipetted into HPLC vials and ran using HPLC with a sample volume of 100 μL. A higher volume of blood and tissue samples injected into the HPLC (100 μL) versus the calibration curve of TEFM180 (**3**) volumes (20 μL) allowed for the detection of smaller quantities of TEFM180 (**3**) in biological samples. To correct for differences in volume between biological samples runs and calibration curve runs, the pharmacokinetics study data were divided by 5.

5.10. [^{3}H]TEFM180 (**10**) autoradiography in rat brain tissue sections

Autoradiography was conducted using [^{3}H]TEFM180 (**10**) on adult male Sprague-Dawley rat brain tissue sections (coronal, 10 μm thick). Sections were cut at different levels from frozen rat brain and thaw-mounted onto slides then stored at –80 °C until use. For estimation of the dissociation constant (K_D), sections were incubated for 180 min at room temperature or 37 °C in 50 mM Tris-HCl (Sigma-Aldrich, USA) buffer with 1 % DMSO (Merck, Germany), pH 7.4, in the presence of 7 different concentrations of [^{3}H]TEFM180 (0.1 nM, 0.5 nM, 1.25 nM, 2.5 nM, 5 nM, 10 nM and 20 nM). Non-specific binding was determined in adjacent section in the presence of 20 μM of TEFM180 (**3**) in 50 mM Tris-HCl buffer with 1 % DMSO, pH 7.4. To end the incubation, slides were washed in Tris HCl (3 × 3 min) and then given a final dip in distilled water (dH_2O). After being left to dry, slides were placed into a cassette and exposed on a tritium imaging plate (BAS-TR2040, FUJIfilm, Japan). The image plates were left in a dark and dry place for 7 days before it was read on the phosphoimager (Typhoon FLA 7000, Biomolecular imager, Cytiva, USA). The imaging plate was imaged using the phosphoimager 4000 V setting with the spatial resolution set to 10 μm. The image generated was saved as a TIFF for later processing and analysis using Fiji image analysis software (NIH, USA). Relative optical density measurements were obtained from whole brain tissue sections at two separate coronal levels. Specific binding was estimated as total binding minus non-specific binding divided by total binding and expressed as a percentage. Then, K_D values were determined by nonlinear regression analysis using GraphPad Prism version 9.3 (GraphPad Software Inc., USA). For characterization of radiotracer regional distribution in the brain as well as estimation of binding potential (*BP*), autoradiography studies were conducted using a total binding stock of 5 nM of [^{3}H]TEFM180 (**10**) (99 % Tris HCl and 1 % DMSO) and a non-specific stock spiked with 20 μM TEFM180 (**3**). The slides were then placed into the total or non-specific solutions for a 3-hour period at room temperature or 37 °C. To end the incubation, slides were washed in Tris HCl (3 × 3 min) and then given a final dip in dH_2O. After being left to dry, slides were placed into a cassette and exposed on a tritium imaging plate (BAS-TR2040, FUJIfilm, Japan). Slides were then imaged as described above and saved as TIFF images for processing using Fiji image analysis

software. Relative optical density measurements were obtained from brain regions defined with reference to a rat brain atlas.[22] Relative optical density measurements were converted to μCi/g using [^{3}H]-standards and a calibration curve. The values were then converted to give an approximated value for $B_{available}$ (expressed in fmol/mg, Eq. (1) and this along with the K_D gave an approximated *BP* (Eq. (2)) for TEFM180 (**3**) in different ROIs.

$$B_{avail}(fmol/mg) = \frac{\text{Binding } (\mu Ci/mg)}{\text{Molar activity } (\mu Ci/nmol)} \times 10^6 \quad (1)$$

where B_{avail} = available binding sites and binding refers to specific binding.

$$BP = \frac{B_{avail}\ (nM)}{K_D(nM)} \quad (2)$$

where *BP* = binding potential and K_D = dissociation constant. B_{avail} was converted from fmol/mg to nM assuming a brain density of 0.99 g/mL.[23]

5.11. Haematoxylin and Eosin (H&E) staining

Slides were placed into 100 % industrial methylated spirit (IMS) for 20 s and subsequently moved through 95 %, 80 % and 75 % IMS, respectively, for 20 s each. Next the slides were placed into haematoxylin for 5 min which was followed by a wash (dipped) in dH_2O. Slides were then placed in acid alcohol for 10 s followed by a wash and then placed into scots tap water solution for 25 s. After another wash, the slides were placed in eosin for 10–12 s and again washed. Excess dH_2O was then removed and the tissue was dehydrated by placing the slides in 70 %, 80 %, 95 %, 100 % and another final 100 % IMS again (20 s each). The slides were then transferred into xylene (2 × 5mins) and then into premountant xylene. After completion PERTEX mountant (Cell Path, UK) was applied to the slide and a cover slip added. The tissue was then inspected under a microscope.

5.12. Radiosynthesis of [^{11}C]TEFM180

Radiochemistry was carried out on a Synthra synthesizer (SYNTHRA Gmbh, Germany, bespoke Wolpertinger modification). No-carrier-added [^{11}C]carbon dioxide was produced on 16.4 MeV GE Healthcare PETtrace cyclotron at the Radiopharmaceutical Unit (RPU) of the West of Scotland PET Centre, Gartnavel Hospital, Glasgow, via the ^{14}N(p,α) ^{11}C nuclear reaction by irradiation of an aluminium target filled with 99.9 % Nitrogen/0.1 % oxygen gas mixture (purchased from BOC, UK) with a beam of protons at 20 μA. Typically after 3 min target irradiation, 10 GBq of [^{11}C]CO_2 was obtained at the End Of Bombardment. The [^{11}C]CO_2 was trapped in a stainless steel loop at − 180 °C and rinsed with He gas. Conversion to [^{11}C]CH_4 took place at 425 °C in an oven filled with an activated Ni catalyst and was then passed through an Ascarite® trap. The [^{11}C]CH_4 was trapped on Carbosphere® at −140 °C and rinsed with He to remove residual H_2 gas. The conversion to [^{11}C]MeI took place by circulating the [^{11}C]CH_4 through an iodine oven heated to 95 °C, then passing through a high temperature oven at 730 °C. The [^{11}C]MeI was separated by trapping on a Porapak Q column® and any residual [^{11}C]CH_4 was circulated in a loop, repeating this process. The [^{11}C]MeI was de-adsorbed at 200 °C by a 10 mL/min flow of He and bubbled into a mixture of 2-hydroxy-6-(mesitylamino)-3-methylbenzamide (**124**) (5.0 mg, 0.017 mmol) and tetra-*n*-butylammonium fluoride (20 μL, 0.020 mmol; 1 M solution in tetrahydrofuran) in cyclohexanone (0.5 mL) at 120 °C for 3 min at a flow rate of 2 mL min^{-1}. The reaction mixture was then diluted with acetonitrile (0.62 mL) and water (0.38 mL) and loaded onto a C_{18} Synergi Hydro-RP 80 Å, 150 × 10 mm, 4 μm column (Phenomenex, UK). A 62 % solution of acetonitrile in water was used as the mobile phase at a flow rate of 5.5 mL min^{-1}. The radiolabelled product was detected by the HPLC gamma-detector and eluted at approximately 32 min. The collected fraction was diluted with water (26 mL) and then transferred onto a Sep-Pak® Plus Light HLB cartridge. This was rinsed with water (10 mL) and the product eluted with ethanol (0.5 mL) then saline (12 mL). This provided a 4 % ethanol/saline formulation of the product in a total synthesis time of 63 min. The radiolabelled product was isolated with an activity yield of 13 % in a total synthesis time of 63 min and a radiochemical purity of >99 %.

Author contributions

The manuscript was written through contributions of all authors. All authors have given approval of the final version of the manuscript.

CRediT authorship contribution statement

Robert C. Shaw: Writing – original draft, Writing – review & editing, Visualization, Validation, Resources, Project administration, Methodology, Investigation, Formal analysis, Data curation. **Timaeus E.F. Morgan:** Writing – review & editing, Resources, Methodology, Investigation, Formal analysis, Data curation. **Holly McErlain:** Project administration, Investigation, Formal analysis. **Carlos J. Alcaide-Corral:** Investigation. **Adam D. Waldman:** Writing – review & editing, Visualization, Supervision, Resources, Funding acquisition. **Dmitry Soloviev:** Investigation, Methodology, Resources, Supervision, Validation, Writing – review & editing. **David Y. Lewis:** Methodology, Resources, Supervision. **Andrew Sutherland:** Writing – review & editing, Writing – original draft, Visualization, Validation, Supervision, Resources, Project administration, Methodology, Investigation, Funding acquisition, Formal analysis, Data curation, Conceptualization. **Adriana A.S. Tavares:** Writing – review & editing, Writing – original draft, Visualization, Validation, Supervision, Software, Resources, Project administration, Methodology, Investigation, Funding acquisition, Formal analysis, Data curation, Conceptualization.

Declaration of competing interest

The authors declare that they have no known competing financial interests or personal relationships that could have appeared to influence the work reported in this paper.

Acknowledgements

Financial support for a SPRINT MS/MND PhD studentship grant to RS, from the Neurosciences Foundation and EPSRC (studentship to TEFM, EP/M506539/1) and from the RS Macdonald Seedcorn Fund (AAST) is gratefully acknowledged. The British Heart Foundation is greatly acknowledged for providing funding towards establishment of the preclinical PET laboratory at the University of Edinburgh (RE/13/3/30183) and radiometabolite laboratories (RG/16/10/32375). AAST and TEFM were funded by the British Heart Foundation (RG/16/10/32375, FS/19/34/34354). AAST is a recipient of a Wellcome Trust Technology Development Award (221295/Z/20/Z). This publication has been made possible in part by CZI grant DAF2021-225273 and grant DOI https://doi.org/10.37921/690910twdfoo from the Chan Zuckerberg Initiative DAF, an advised fund of Silicon Valley Community Foundation (funder DOI 10.13039/100014989). CA-C is supported by the Edinburgh Preclinical Imaging. The authors are grateful to the Little France BVS staff for invaluable support to the project.

Appendix A. Supplementary data

HPLC trace of TEFM180 as well as [^{11}C]TEFM180, ^{1}H and ^{13}C NMR spectra of all compounds. This material is available free of charge via the Internet at https://pubs.acs.org. Supplementary data to this article can be found online at https://doi.org/10.1016/j.bmc.2024.118057.

Data availability

Data will be made available on request.

References

1. Rae-Grant A, Day GS, Marrie RA, et al. Practice guideline recommendations summary: Disease-modifying therapies for adults with multiple sclerosis. *Neurology*. 2018;90:777–788.
2. Published CU. Ocrelizumab for treating primary progressive multiple sclerosis. 2018;(June):1–19. Available from: https://www.nice.org.uk/guidance/TA585.
3. Ransohoff RM, Hafler DA, Lucchinetti CF. Multiple sclerosis - A quiet revolution. *Nat Rev Neurol*. 2015;11:134–142.
4. Malek RL, Toman RE, Edsall LC, et al. Nrg-1 belongs to the endothelial differentiation gene family of G protein-coupled sphingosine-1-phosphate receptors. *J Biol Chem*. 2001;276:5692–5699.
5. Beer MS, Stanton JA, Salim K, et al. EDG receptors as a therapeutic target in the nervous system. Available from *Ann N Y Acad Sci [internet]*. 2000;905:118–131. http://www.scopus.com/inward/record.url?eid=2-s2.0-0034093521&partnerID=tZOtx3y1.
6. Chun J, Hla T, Lynch KR, Spiegel S, Moolenaar WH. International union of basic and clinical pharmacology. LXXVIII Lysophospholipid. *Pharmacol Rev*. 2010;62:579–587.
7. Im DS, Clemens J, Macdonald TL, Lynch KR. Characterization of the human and mouse sphingosine 1-phosphate receptor, S1P5 (Edg-8): structure–activity relationship of sphingosine1-phosphate receptors. *Biochemistry*. 2001;40:14053–14060.
8. Terai K, Soga T, Takahashi M, et al. Edg-8 receptors are preferentially expressed in oligodendrocyte lineage cells of the rat CNS. *Neuroscience*. 2003;116:1053–1062.
9. Jaillard C. Edg8/S1P5: an oligodendroglial receptor with dual function on process retraction and cell survival. Available from *J Neurosci [Internet]*. 2005;25:1459–1469. http://www.jneurosci.org/cgi/doi/10.1523/JNEUROSCI.4645-04.2005.
10. Townsend D, Cheng Z, Georg D, Drexler W, Moser E. Grand challenges in biomedical physics. *Front Phys*. 2013;1:1–6.
11. Mattes H, Dev KK, Bouhelal R, et al. Design and synthesis of selective and potent orally active S1P5 agonists. *ChemMedChem*. 2010;5:1693–1696.
12. Hulme EC, Trevethick MA. Ligand binding assays at equilibrium: Validation and interpretation. *Br J Pharmacol*. 2010;161:1219–1237.
13. Mock B. Automated C-11 methyl iodide/triflate production: current state of the art. *Curr Org Chem*. 2013 Oct 1;17:2119–2126.
14. Tavares A, Becker G, Barret O, et al.. Initial evaluation of [18F]F13714, a novel 5-HT1A receptor agonist in non-human primates. In: Annual Congress of the European Association of Nuclear Medicine [Internet]. 2013. Available from: https://hal.science/hal-00948404.
15. Chun J, Hartung HP. Mechanism of action of oral fingolimod (FTY720) in multiple sclerosis. *Clin Neuropharmacol*. 2010;33:91–101.
16. Shaw RC, Tamagnan GD, Tavares AAS. Rapidly (and successfully) translating novel brain radiotracers from animal research into clinical use. *Front Neurosci*. 2020;14:1–18.
17. Pike VW. PET radiotracers: crossing the blood-brain barrier and surviving metabolism. *Trends Pharmacol Sci*. 2009;30:431–440.
18. Pike VW. Positron-emitting radioligands for studies in vivo - Probes for human. *J Psychopharmacol*. 1993;7:139–158.
19. Laruelle M, Slifstein M, Huang Y. Relationships between radiotracer properties and image quality in molecular imaging of the brain with positron emission tomography. *Mol Imag Biol*. 2003;5:363–375.
20. Briard E, Orain D, Beerli C, et al. BZM055, an iodinated radiotracer candidate for PET and SPECT imaging of myelin and FTY720 brain distribution. *ChemMedChem*. 2011;6:667–677.
21. Bennett CN, Horrobin DF. Gene targets related to phospholipid and fatty acid metabolism in schizophrenia and other psychiatric disorders: an update. *Prostaglandins Leukot Essent Fat Acids*. 2000;63:47–59.
22. Herman JP, Watson SJ. The rat brain in stereotaxic coordinates (2nd edn). Vol. 10, Trends in Neurosciences. 1987. 439 p.
23. Beckmann F, Heise K, Kölsch B, et al. Three-dimensional imaging of nerve tissue by X-ray phase-contrast microtomography. *Biophys J*. 1999;76:98–102.